

Switchable Holographic Polymer-Dispersed Liquid Crystal Reflection Gratings Based on Thiol–Ene Photopolymerization

Lalgudi V. Natarajan,^{*,†} Christina K. Shepherd,[†] Donna M. Brandelik,[†]
Richard L. Sutherland,[†] Suresh Chandra,[†] Vincent P. Tondiglia,[†]
David Tomlin,[‡] and Timothy J. Bunning^{*,§}

Air Force Research Laboratory, Materials and Manufacturing Directorate/MLPJ,
Wright-Patterson AFB, Ohio 45433, Science Applications International Corporation,
4031 Colonel Glenn Highway, Dayton, Ohio 45431, and Technical Management Concepts Inc.,
Beavercreek, Ohio 45433

Received January 10, 2003. Revised Manuscript Received April 22, 2003

Holographic reflection gratings in polymer-dispersed liquid crystals (H-PDLCs) were formed by thiol–ene photopolymerization. Using UV laser light and a single prism, electrically switchable reflection gratings in blue, green, yellow, and red colors were fabricated. Results indicate that thiol–ene polymers function as better hosts for H-PDLC than multifunctional acrylate as matrixes. These differences are the result of a much different temporal structure development caused by fundamental differences in the polymerization propagation mechanism: a step-growth addition mechanism for the thiol–ene system compared to a chain-growth addition mechanism in multifunctional acrylates. Morphology studies by TEM support these conclusions, as striking differences in droplet shape and uniformity are observed. Discrete nematic droplets with a nearly spherical shape were seen. Thiol–ene polymers offer lower switching fields, higher diffraction efficiencies, better optical properties, and higher thermal stabilities. The response times of the thiol–ene gratings were five times slower than those of acrylates.

Introduction

Holographic polymer-dispersed liquid crystals (H-PDLCs) formed by nonhomogeneous spatial illumination of monomer/LC mixtures have been the center of much research lately.^{1–3} An anisotropic distribution of polymer and LC-rich lamellae in these films gives rise to a periodic refractive index modulation that can be modulated electrically. The dynamic nature of the gratings has high potential for devices in display technology and communications.⁴ H-PDLC films exhibit high switching fields (~ 10 V/ μm), high contrast ratios,

good transmission in the on and off states, and switching speeds on the order of microseconds.

For several years, the focus of research in H-PDLCs has been on highly cross-linked acrylate polymer systems.^{1–3} However, multifunctional acrylates as hosts for H-PDLC gratings have some drawbacks. Because final monomer conversion is low as a result of early gelation and subsequent vitrification, polymerization can continue after grating formation for extended periods of time, even in the dark. This leads to an increase over time in the switching field needed to modulate the refractive index.⁵ Also observed is substantial shrinkage ($> 3\%$) during exposure, as evidenced by a blue shift of the notch.⁶ This blue shift appears immediately upon recording and continues to develop over a few days, yielding a total shrinkage of typically 5%. Asymmetric notch shapes, which have been related to nonuniform shrinkage (spatially different across the grating) within the films, are also observed in these systems. This chirping of the refractive index profile ultimately limits the peak diffraction efficiency.⁶ The large distribution of droplet shapes and interconnectivity typical in a rapidly gelling system also diminishes the sharpness of the electrical switching and increases

* To whom correspondence to be addressed. Tel.: (937) 255-3808. Fax: (937) 255-1128. E-mail: Lalgudi.Natarajan@wpafb.af.mil (L.V.N.), Timothy.Bunning@wpafb.af.mil (T.J.B.)

[†] Science Applications International Corporation.

[‡] Technical Management Concepts Inc.

[§] Wright-Patterson AFB.

(1) Bunning, T. J.; Natarajan, L. V.; Sutherland, R. L.; Tondiglia, V. P. *Annu. Rev. Mater. Sci.* **2000**, *30*, 83.

(2) Sutherland, R. L.; Natarajan, L. V.; Tondiglia, V. P.; Bunning, T. J. *Handbook of Advanced Electronic and Photonic Materials and Devices*; Nalwa, H. S., Ed.; Academic Press, San Diego, 2000; Vol. 7, Switchable Holographic Polymer-Dispersed Liquid Crystals, pp 68–103.

(3) (a) Crawford, G. P.; Fiske, T. G.; Silverstein, L. S. In *SID Digest of Technical Papers*; Society for Information Display (SID): San Jose, CA, 1998; p 127. (b) Bowley, C. C.; Crawford, G. P. *J. Opt. Technol.* **2000**, *67*, 717. (c) Bowley, C. C.; Kossyrev, P. A.; Crawford, G. P.; Faris, S. *Appl. Phys. Lett.* **2001**, *79*, 9.

(4) (a) Sutherland, R. L.; Bunning, T. J.; Natarajan, L. V.; Tondiglia, V. P.; Siwecki, S. A.; Chandra, S. *SPIE Proc.* **2001**, *4463*, 1. (b) Tanaka, K.; Kato, K.; Tsuru, S.; Sakai, S. *J. Soc. Inf. Display* **1994**, *2*, 37. (c) Domash, L. H.; Crawford, G. P.; Ashmead, A. C.; Smith, R. T.; Popovich, M. M.; Storey, J. *SPIE Proc.* **2000**, *4107*, 46.

(5) Klosterman, A. M.; Pogue, R. T.; Schmitt, M. G.; Natarajan, L. V.; Tondiglia, V. P.; Tomlin, D.; Sutherland, R. L.; Bunning, T. J. *MRS Proc.* **1999**, *559*, 129.

(6) Sutherland, R. L.; Tondiglia, V. P.; Natarajan, L. V.; Bunning, T. J. *Appl. Phys. Lett.* **2001**, *79*, 1420.

unwanted optical scattering due to the increased interfacial area.

It should be noted that, in most visibly recorded H-PDLCs to date, a number of additives typically are required.¹ First, a visible initiator and sometimes a co-initiator are added to provide an initiation path. Second, the viscosity of these multifunctional acrylate syrups is typically high, and to ensure good homogeneous mixing, a reactive solubilizer such as *N*-vinyl pyrrolidinone is added.^{1–3} Third, because most of these systems have high switching voltages because of their very small-sized and irregular-shaped domains, surfactant-like molecules are typically added to reduce the strong anchoring interactions of the droplet with the host polymer. Although this addition reduces the switching fields substantially,^{7,8} it also leads to undesirable heating effects when an electric field is applied.⁹ All of these additives are potential sources of contamination in the LC droplets, causing a decrease in the clearing temperature and order parameter. Over time, these small molecules can also leach into the LC domains, causing long-term changes in the optical and electrooptical properties of the gratings.

Thiol–ene polymers are well-known for their role in the preparation of UV-curable coatings and adhesives.¹⁰ The polymers formed are more elastic and offer better adhesion than those containing only acrylate-based precursors. Thiol–ene polymers are formed by the combination of step-growth and free-radical reactions between multifunctional aliphatic thiols and vinyl monomers containing “ene” groups. Photoinitiation to produce free-radical centers is the best known method of polymerization. However, growth of the molecular weight occurs stepwise, as in a condensation reaction. The thiol–ene reaction is based on a stoichiometric relation between the reacting components: either the thiol or the ene must have a functionality of >2 for polymer formation and cross-linking. The thiol–ene reaction mechanisms, polymerization kinetics, and reactivities of different thiol systems have been reviewed by Jacobine.¹⁰

Another significant difference between thiol–ene and acrylate polymerization is the reactivity of the systems in the presence of oxygen. Acrylate polymerization is strongly inhibited by oxygen, unlike thiol–ene polymerization, where oxygen is incorporated into the growing polymer chains as a peroxy radical that undergoes chain transfer with a thiol to regenerate the thiyl radical. Although the photoinitiator efficiency decreases slightly as a result of the quenching of the triplet excited state, overall, the polymerization rate is not significantly altered. Another interesting aspect of thiol–ene polymerizations is that the reaction can be carried out in the absence of a photoinitiator. It is possible to directly photolyze thiol units by cleavage of the S–H bond to give a thiyl radical and hydrogen atom, which initiates the polymerization.¹¹ This high reactivity typically

necessitates the addition of a stabilizer to increase the shelf life of thiol–ene monomers. Other advantages of thiol–ene monomers include low toxicity and reduced nonuniform shrinkage relative to multifunctional acrylate monomers. This latter attribute is a direct result of the step-growth polymerization mechanism, which results in higher conversions at much lower viscosities later in the reaction time than are found in chain-growth acrylate systems.

In any polymerization mechanism where van der Waal distances between reactive groups are converted to covalent bonds, a microscopic free volume loss results, which translates into bulk shrinkage. For a step-growth system, conversion is related to the functionality of the monomer, and for typical thiol–ene systems, the gel point does not occur until conversions exceed 50%. Because of the late gelation in thiol–ene systems, polymerization can be driven to almost 100% conversion in ene double bonds, and because most of the double bonds are consumed while the precursors are in the liquid state, the adverse consequences of shrinkage are not manifested in the films.¹⁰ Shrinkage in these systems that occurs before the gel point is reached can be readily accommodated by the liquid mixture of oligomers. This is contrary to conventional chain-growth reactions of highly functional acrylic monomers, where gelation occurs very early in the reaction ($<5\%$ conversion). Once the gel is established, further conversion leads to volumetric shrinkage that is transferred to the network because it cannot be easily accommodated. In conventional multifunctional acrylates, double-bond conversion decreases with functionality, and shrinkage of $>10\%$ is observed.¹²

The use of both thiol–ene and acrylate monomers as hosts for the phase separation of nematic liquid crystals in conventional polymer-dispersed liquid crystals has been well documented.⁹ In both cases, high-molecular-weight polymer is formed, and therefore, phase separation takes place, resulting in a two-phase composite whose optical properties can be electrically modulated. Although a wide range of nematic droplet morphologies can be produced depending on the intensity and LC concentration, there are typically large differences in the two-phase morphologies between these two monomer types. The acrylate systems typically contain a heterogeneous droplet size and shape (nonspherical) distribution, whereas thiol–ene systems exhibit spherical and monodisperse domains.⁹ These differences are due to differences in the evolution of the molecular weight (MW) as a function of time between the two systems. In acrylates, where high-MW polymer is formed immediately, gelation typically precedes phase separation.¹³ In thiol–enes, the MW increases in a stepwise fashion, and phase separation precedes gelation.¹⁴

(7) Natarajan, L. V.; Sutherland, R. L.; Tondiglia, V. P.; Bunning, T. J.; Adams, W. W. *J. Non-Opt. Phys. Mat.* **1996**, *5*, 89.

(8) Tondiglia, V. P.; Natarajan, L. V.; Sutherland, R. L.; Neal, R. M.; Bunning, T. J. *MRS Proc.* **1998**, *479*, 235.

(9) Drzaic, P. S. In *Liquid Crystal Dispersions*; World Scientific: Singapore, 1995; pp 30–59.

(10) Jacobine, A. F. In *Radiation Curing in Polymer Science and Technology III*; Fouassier, J. D., Rabek, J. F., Eds.; Elsevier Applied Science: London, 1993; Chapter 7, p 219.

(11) Hoyle, C.; Cole, M. C.; Viswanathan, K.; Nguyen, C.; Kuang, W.; Bowman, C.; Cramer, N.; Jonasson, S.; Viswanathan, K. In *RadTech Technical Conference Proceedings*; RadTech: Chevy Chase, MD, 2000; pp 211–220.

(12) Sathir, R. K.; Luck, R. M. *Expanding Monomers: Synthesis, Characterization And Applications*; CRC Press: Boca Raton, FL, 1992; Chapter 1, pp 1–50.

(13) (a) Boots, H. M. J.; Kloosterboer, J. G.; Serbutoviez, C.; Touwslager, F. J. *Macromolecules* **1996**, *29*, 7683. (b) Serbutoviez, C.; Kloosterboer, J. G.; Boots, H. M. J.; Touwslager, F. J. *Macromolecules* **1996**, *29*, 7690.

There are only few reports on thiol–ene-based H-PDLC reflection gratings. Date et al.¹⁵ reported H-PDLC reflection gratings obtained by using a combination of commercially available NOA65 and NOA68 mixtures. Gratings were written at visible wavelengths using an Ar ion laser. No detailed study of the morphology or the stability of the grating performances were reported. Curing of pure thiol–ene systems in the visible region without acrylate monomers is difficult because of the interaction of the thiol–ene chemistry with the visible initiator. Curing using UV radiation for H-PDLC reflection gratings has not been examined in any detail. This has been due, in part, to the need for a large, coherent, high-power source of UV radiation and the associated optics. Although we were successful in writing transmission gratings in NOA 65, our earlier attempts to write reflection gratings with a UV laser were not fruitful.¹⁶

In this paper, we report on the results of a detailed study of the optical, electrooptical, and morphological properties of H-PDLC reflection gratings produced by UV-initiated holographic photopolymerization of thiol–ene monomers. The addition of a more powerful initiator to NOA 65 and the use of a higher-power ($>50\text{mW}/\text{cm}^2$, 364 nm) UV laser allowed for the formation of a permanent reflection grating with good diffraction efficiency (DE). No additives other than a UV initiator are needed. A simple single-prism technique was used for writing. Our gratings demonstrate improved performance with respect to multifunctional acrylates, including lower nonuniform shrinkage, better long-term stability, and less complex syrup formulations.

Experimental Section

Both a commercially available thiol–ene formulation from Norland Inc., NOA 65, and a formulation containing pentaerythritol tetrakis(3-mercaptopropionate) (PETMP) (Aldrich) and trimethylol propane diallyl ether (TMPDE) (Aldrich) were employed (Figure 1). No significant differences in the grating performance were seen between the two formulations. Although the commercial material NOA 65 has a proprietary UV initiator, only weak reflection gratings with $\text{DE} < 20\%$ could be obtained. The addition of Irgacure 1173 UV initiator (0.1%) greatly enhances the DE ($>70\%$) for the same UV power. Thin sample cells were made using $8\text{-}\mu\text{m}$ spacers. Both glass and ITO glass slides were used. The prepolymer formulation consisted of aliphatic thiol and allyl ether in equimolar concentrations and 30–32% nematic liquid crystal BL037 (EMerck) with 0.1% Irgacure 1173 UV initiator. For comparison, a pentaacrylate formulation consisting of dipentaerythritol hydroxy penta acrylate from Aldrich Co. was used. Writing of the grating was done using a Coherent Ar-ion laser (model 308C) with a laser wavelength of 363.8 nm and an output power of $\sim 200\text{ mW}$. The laser cavity did not include any etalon, and therefore, the laser coherence length was only about 1 cm. The UV laser beam was expanded to 5 mm indiameter using a $4\times$ microscope objective. The gratings were written in a single-beam configuration. The reflection grating was formed as a result of interference between the incident beam and its own total internal reflection, as shown in the Figure 2. An isosceles 90° glass prism was used for holographic writing. The cell was placed in optical contact with the prism hypotenuse using an index-matching fluid. The exposure time was typi-

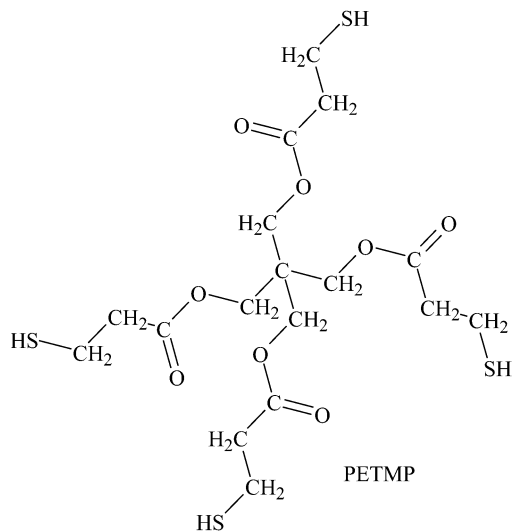
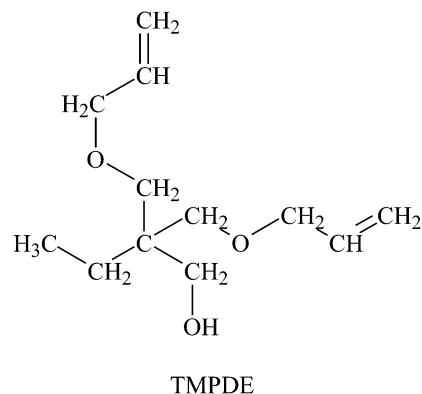


Figure 1. Chemical structures of the multifunctional thiol (PETMP) and diallyl ether (TMPDE).

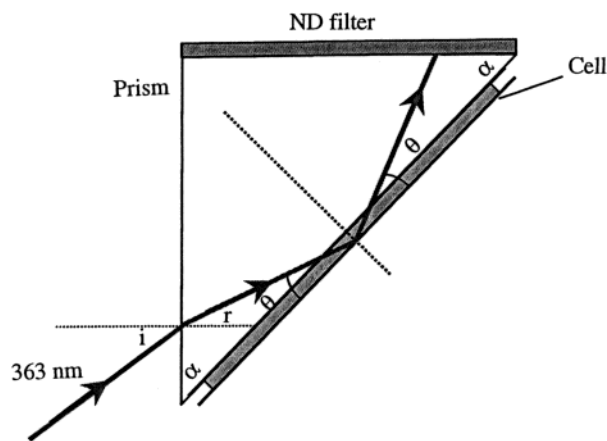


Figure 2. Writing geometry, showing the single beam incident on the prism attached to the cell.

cally 10 s. With $i = 0^\circ$ (normal incidence at entrance face and 45° angle of incidence at the cell), the observed grating notch occurred at a wavelength of 470 nm. The prism and the cell assembly were placed on a rotation stage so that the notch wavelength could be changed easily. Gratings at other notch wavelengths, including green, yellow, and red ones, could then be selected by simply turning the rotation stage appropriately.

Bright-field transmission electron microscopy (BFTEM) was performed on a FEI CM200FEG TEM on unstained 50–60-nm sections. Ultramicrotomy was performed at room temperature on a Reichert ultracut utilizing a diatome 35° diamond knife. Optical characterization of the reflection gratings was carried out using an Ocean Optics fiber spectrometer. A white

(14) Yamagashi, F. G.; Miller, L. J.; Van Ast, C. I. *SPIE Proc.* **1989**, 1080, 24.

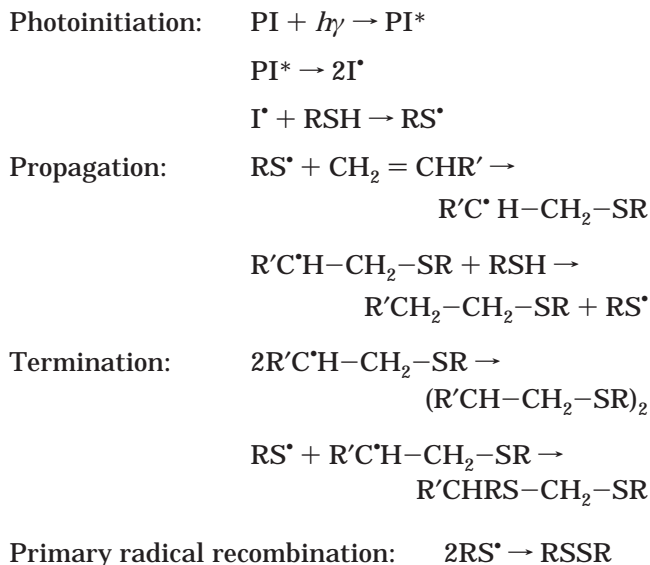
(15) Date, M.; Takeuchi, Y.; Tanaka, K.; Kato, S. *J. Soc. Inf. Display* **1998**, 6, 37.

(16) Sutherland, R. L. *SPIE Proc.* **1989**, 1080, 83.

light source coupled to a fiber-optic delivery system was used as the light source. For electrical switching, a square-wave signal at 1 kHz operating from 0 to 200 V RMS was applied, and the changes in reflection efficiency were noted. The switching time of the reflection hologram was measured by directing the reflection from the grating into a fast PIN photodiode connected to an oscilloscope. A positive dc pulse of 125 V with a duration of 2 ms was applied. The switching time was measured by following the 10 to 90% change in the reflection intensity.

Results and Discussion

The mechanism of thiol-ene polymerization is well documented in the literature^{10,17} and can be described as occurring in the following steps: The commercial UV initiator Irgacure 1173 (1-phenyl-2-hydroxy-2-methylpropan-1-one) is excited by UV radiation and cleaves into radical centers capable of initiating polymerization. The radical produced from 1-phenyl-2-hydroxy-2-methylpropan-1-one will initiate the polymerization by abstracting hydrogen from the thiol or by directly adding to the ene double bond. Termination by the three reactions shown below is likely.



It is reasonable to assume that the thiol and the allyl ether in stoichiometric amounts will be consumed at similar rates.¹⁰ It is our reasoning that very high concentrations of free radicals in a short exposure time are needed to accelerate the polymerization and cause phase separation leading to the formation of nematic droplets with sizes <100 nm. The grating spacings of the blue, green, and red gratings are on the order of 0.13–0.21 μm . Upon UV excitation, Irgacure 1173 and other related UV initiators such as Irgacure 369 yield more than one free radical per molecule. Inefficient UV initiators such as benzophenone give only cloudy samples, suggesting the formation of large droplets that wash out the gratings.

Reflection gratings at several wavelengths across the visible spectrum were easily formed using the thiol-ene formulation. The single-beam/prism combination simplifies the making of holograms, and concerns about the overlap of the beams and vibration effects are

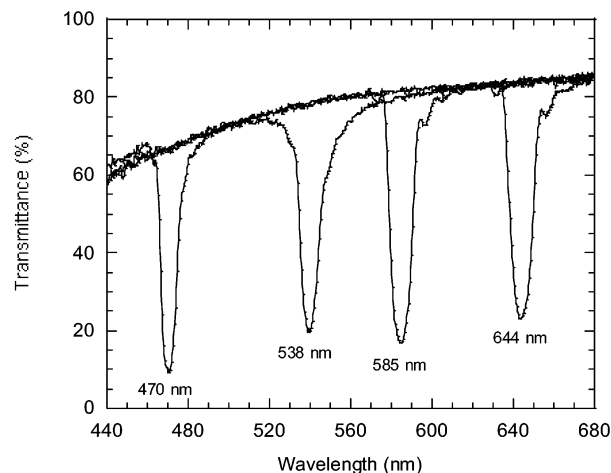


Figure 3. H-PDLC thiol-ene reflection gratings in blue, green, yellow, and red colors.

nonexistent. Figure 3 shows typical reflection gratings with notches at several colors. Measured diffraction efficiencies in the blue and green spectral regions ($\sim 70\%$) were comparable to the best values observed for multifunctional acrylates.¹⁸ No significant polarization dependence of DE was observed. In acrylate systems, DE for P polarization is higher than DE for S polarization by a few percent.¹⁹

For acrylates as H-PDLC hosts, we observed a progressive blue shift of the reflection notch during real-time monitoring of grating formation.^{6,20} We attribute the blue shift to polymer shrinkage during the curing process. According to the Bragg relation, an expected increase of the polymer refractive index due to curing should red shift the notch; thus, any blue shift observed gives a low estimate of the amount of shrinkage. The blue shift is due to the reduction of the optical thickness (grating spacing) as a result of the physical shrinkage of the polymer. The shrinkage during grating formation was $\sim 3\%$. An estimate of the shrinkage in thiol-ene systems was not made, as real-time experiments have not yet been carried out. Determination of the shrinkage value requires knowledge of the refractive indices of the prepolymer syrup at the writing wavelength, 364.8 nm, and of the cured polymer at different Bragg wavelengths. Experimental determinations of the refractive index of the uncured syrup at the UV recording wavelength are more problematic because of the onset of curing when the syrup is irradiated with UV light. A detailed examination of the shrinkage will be part of a future study. The symmetrical nature and the narrow bandwidth (<15 nm) of the notch are indicative of a more uniform shrinkage during writing (Figure 3) than for multifunctional acrylates. In the latter materials, considerable chirping and broadening of the notch is observed, suggesting nonuniform shrinkage.⁴ Because of the difference in gel point with respect to conversion, it is expected that the effect of shrinkage on the notch

(18) Natarajan, L. V.; Sutherland, R. L.; Tondiglia, V. P.; Bunning, T. J. *MRS Proc.* **1999**, 559, 108.

(19) (a) Sutherland, R. L. *J. Opt. Soc. Am. B* **2002**, 19, 2995. (b) Sutherland, R. L.; Natarajan, L. V.; Bunning, T. J.; Tondiglia, V. P.; Brandelik, D.; Shepherd, C. K.; Chandra, S.; Siwecki, S. *J. Opt. Soc. Am. B* **2002**, 19, 3004.

(20) Warren, G. T.; DeSarkar, M.; Qi, J.; Crawford, G. P. In *SID Digest of Technical Papers*; Society for Information Display (SID): San Jose, CA, 2001; p 866.

(17) Cramer, N. B.; Bowman, C. N. *J. Polym. Chem. A* **2001**, 39, 3311.

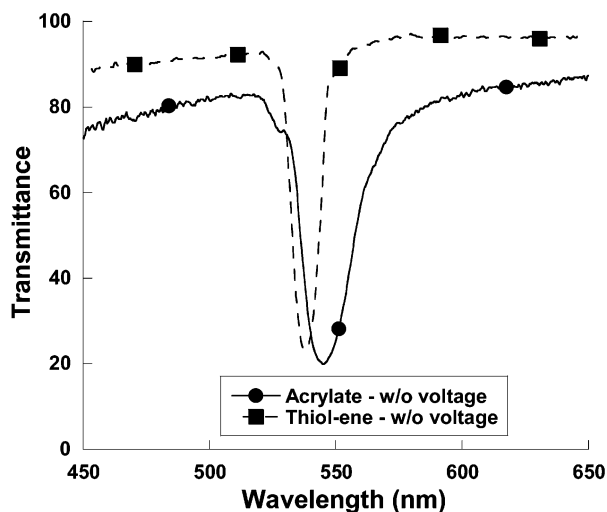


Figure 4. Baseline transmittance of the thiol–ene and acrylate reflection gratings with the field off (notch present).

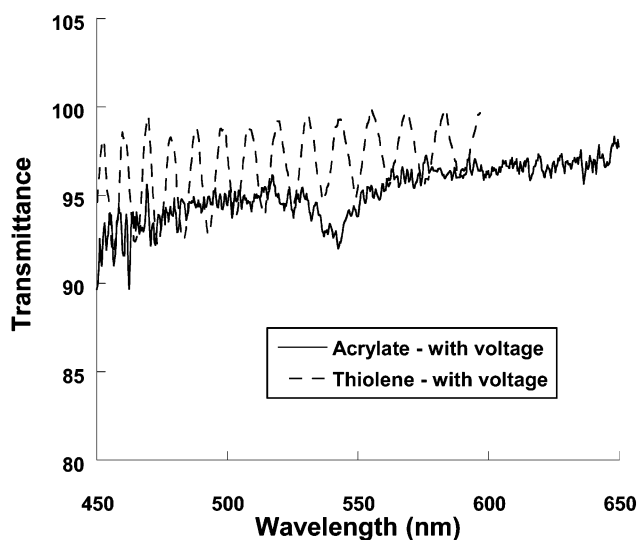


Figure 5. Baseline transmittance of the thiol–ene and acrylate reflection gratings with the field on (notch removed). The oscillations present in the thiol–ene cell are due to interference between substrates caused by the cell design.

wavelength would be much less for the thiol–ene systems.

A direct comparison of the optical properties of comparably written reflection gratings with the two different formulations (thiol–ene and acrylate) is shown in Figures 4 and 5. With the notch present (voltage off), as shown in Figure 4, a large difference in the notch properties is observed. For the thiol–ene system, the notch is narrower, and the asymmetry observed (see the small satellite shoulder on the blue side of the acrylate notch) is greatly diminished. The baseline transmittance at wavelengths outside the notch is also considerably higher (>90%). This implies better homogeneity and thus less scatter in the grating structure. The baseline transmittance without the notch present (voltage on) for the thiol–ene system was greater than 90%, implying good matching of refractive indices of the host polymer and the LC, as shown in Figure 5. In a stacked red, green, blue sample for display applications, these higher transmittance values will be key.

To investigate the interior morphology of these H-PDLC gratings, samples were probed in detail with

TEM and scanning transmission electron microscopy (STEM). Studying the thiol–ene gratings by low-voltage SEM, typically used for H-PDLC grating morphology characterization, was challenging, as the film's elasticity made the typical fracture and mounting steps very difficult. Therefore, both BFTEM and STEM were used to investigate the morphologies. The BF TEM images in Figures 6 (a–d) and 7 (a, b) reveal a different morphology for the thiol–ene samples. Unlike the acrylate systems where very irregular surfaces are observed at the interface between the droplets and polymer, the thiol–ene system interface was very smooth. This irregularity in the interface of the acrylate system has been observed before.²¹ The droplets are similar in shape, and in the cross-sectional plane observed, all resemble slightly distorted spheres. In a direction perpendicular to the TEM micrograph, the size of the domains also appears to be larger, as the sections typically bisect only one droplet in the case of the thiol–ene system. This is different than the acrylate case, where droplets can be observed to be cut throughout the thickness of the section. Both systems exhibit a high fill fraction within the LC-rich lamellae.

This difference in morphology was first explained by Yamagishi.¹⁴ As polymerization takes place in a PIPS system, the initial syrup consisting of monomer and LC is joined by polymer. At the point of phase separation, two phases exist, one rich in LC, monomer (M), and a small fraction of polymer (P) and the other rich in P with small fractions of M and LC. The discontinuous phase, which is key to determining the morphology, can be composed of either phase. Although highly dependent on concentration, the nature of the polymerization mechanism dictates to a large degree which phase is discontinuous. Multifunctional acrylates polymerize via a chain-growth mechanism where monomer is successively added to a rapidly growing chain. High-MW polymer is formed almost immediately, and the monomer concentration decreases steadily with time; monomer is present until the polymerization is complete (100% conversion). Because the high-MW polymer formed has limited solubility in the M/LC syrup, it phase separates early on and becomes the P-rich discontinuous phase. These small P-rich nodes (not a liquid) continue to grow via surface reactive groups and ultimately become attached to one another. In a high-functionality chain-growth system, diffusion-limited reaction kinetics dominate early, and as a result, irregularly shaped domains are formed because of the local heterogeneity of the phase separation process. The LC/M-rich phase resides in these interstitial areas.

In the case of the thiol–ene systems, even though the initial steps involve free-radical addition processes, a step-growth propagation mechanism is dominant, similar to thermally cured epoxy systems. The MW of the polymer increases slowly, and monomer is converted to oligomers early in the reaction. As the number of oligomers increases above a critical concentration, phase separation of an oligomer-rich liquid from an LC-rich liquid occurs. Because both phases are liquid and the viscosity is low, the discontinuous phase typically is spherical in shape as a result of surface tension effects.

(21) Bunning, T. J.; Natarajan, L. V.; Tondiglia, V. P.; Sutherland, R. L.; Vezie, D. L.; Adams, W. W. *Polymer* **1996**, *37*, 3147.

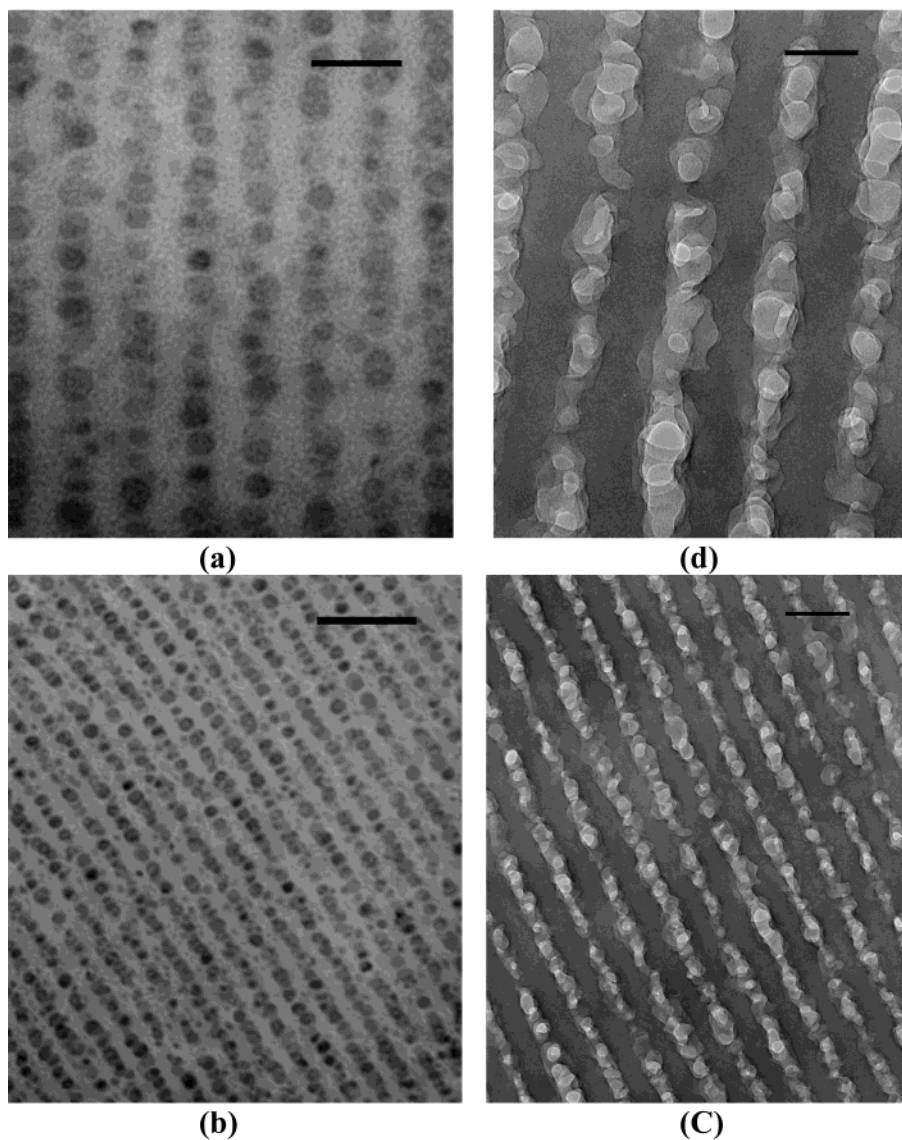


Figure 6. Bright-field transmission electron micrographs of thiol-ene reflection gratings are shown in a and b. Scale bars correspond to (a) 250 and (b) 600 nm. Comparable periodicity acrylate reflection gratings are shown in c and d. Scale bars correspond to (c) 220 and (d) 110 nm.

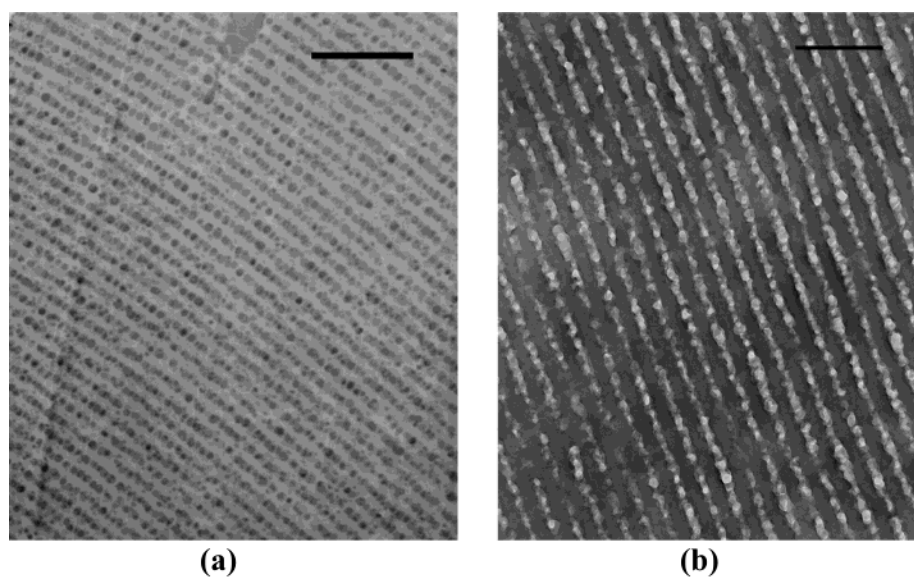


Figure 7. Bright-field transmission electron micrographs at lower magnifications for (a) thiol-ene reflection gratings and (b) acrylate reflection gratings. Scale bars correspond to (a) 1000 and (b) 550 nm

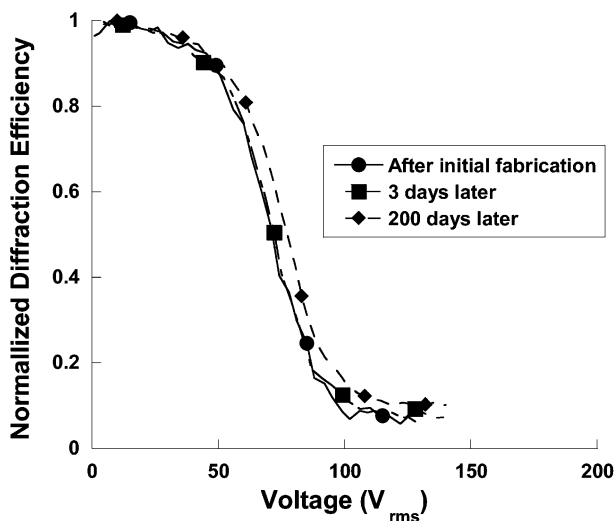


Figure 8. Electrical switching behavior (diffraction efficiency versus voltage) of thiol–ene reflection gratings with aging.

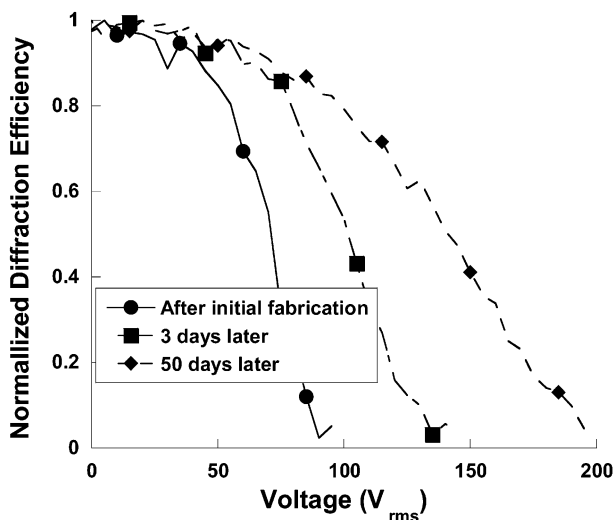


Figure 9. Electrical switching behavior (diffraction efficiency versus voltage) of acrylate reflection gratings with aging.

As the reaction progresses, at some point, the growing oligomeric (polymeric) phase vitrifies and traps the spherical domains in what is classically termed the “swiss cheese” morphology. Our observations are consistent with this explanation. Flood-lit systems formed from both monomer types with equal concentrations of liquid crystal clearly indicate a tendency for the thiol–ene samples to exhibit this classic morphology whereas the multifunctional acrylate systems exhibit a polymer-ball or bicontinuous morphology.¹⁴

The electrooptical properties of the thiol–ene-based systems are stable over long periods of time, as shown in Figure 8, unlike the multifunctional acrylate-based systems shown in Figure 9. No significant changes in DE, notch wavelength, or switching voltage were observed after 200 days for the thiol–ene system. This is contrary to the multifunctional acrylate systems, where substantial post-polymerization effects were present. Some of these are due to continued dark reaction: given only a 50% conversion because of rapid vitrification, a substantial number of double bonds are present that can react slowly over time. The rapid gelation also traps a considerable amount of stress in the system. The fast gelation freezes a nonequilibrium network, which, over

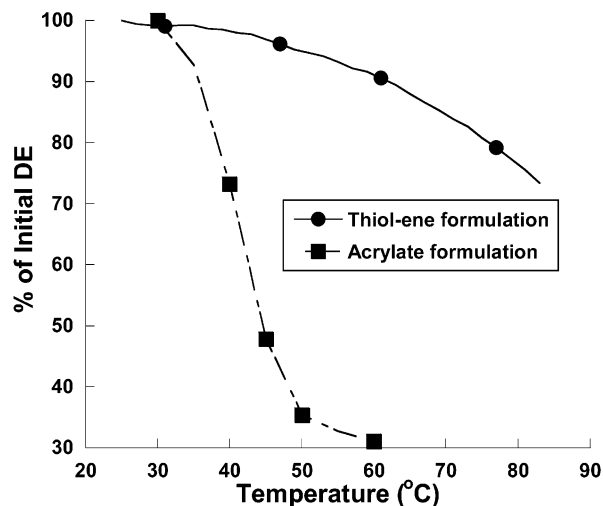


Figure 10. Effect of heating on the diffraction efficiency of the reflection gratings.

time, tries to equilibrate by stress relaxation via molecular motion. Such post-illumination effects seem to be absent in thiol–ene gratings, as shown by the data in Figure 8. We speculate that this is due to the much higher conversion obtained in the thiol–ene systems. Because all of the reactive double bonds are consumed, nothing exists to continue slow dark reactions, and the late gelation (at conversion approaching 100%) eliminates large stresses.

Also indicated in Figure 8 are the much lower switching fields obtained with the thiol–ene systems. We note that a surfactant has been added to the multifunctional acrylate system to reduce surface anchoring interactions; otherwise, switching voltages would be above the 200-V range. This large reduction in the case of thiol–enes might be due to two separate effects, including a change in the inherent morphology and chemical differences at the interface that reduce the anchoring strength. The more elastic nature of the thiol–ene polymer would discourage strong interactions and anchoring of the droplets at the polymer interface.²² A much smoother interface also reduces the surface/volume ratio for domains of equal average diameter. An extensive analysis as to the exact cause is beyond the scope of the present work. Contributions from both effects are likely. Morphological effects that are pertinent include the slightly larger droplet sizes observed in the reflection grating studies. According to the model developed by Wu and Doane,²³ the critical field for switching decreases significantly for larger, more spherical droplets. Larger droplets are also expected to be slower in responding to the field. The measured response times for thiol–ene gratings switching were higher: on and off times on the order of 550 and 1200 μs were observed. Acrylates as hosts exhibited faster response times on the order of 100 and 250 μs for on and off times, respectively.¹⁸ Hence, a reduction of the switching voltage and an increase in switching speeds might result from the combination of a larger droplet size, a more spherical domain shape, and a decreased surface interaction.

(22) Smith, G. W.; Vaz, N. A.; Vansteenkiste. *Mol. Cryst. Liq. Cryst.* **1989**, *174*, 49.

(23) Wu, G.; Erdmann, J. H.; and Doane, J. W. *Liq. Cryst.* **1989**, *5*, 1453.

Thiol-ene polymers as hosts also appear to offer improved thermal stability of the gratings. Heating these films to 80 °C results in a loss of only 20% in DE, whereas, for acrylates, the DE falls sharply at temperatures >40 °C, as shown in Figure 10. At 60 °C, the acrylate grating almost disappears. Although thermal variation of the refractive indices n_0 and n_e might account for some of the decrease, the contamination of the droplets by the large number of additives in the case of acrylates most likely contributes to the large decrease in the clearing temperature of the liquid crystal. These additives are not necessary in the thiol-ene-based systems, and hence, thiol-ene-based systems exhibit superior thermal stability.

Conclusion

We have demonstrated that visible H-PDLC reflection gratings can be recorded in a thiol-ene-based polymer system using a single UV line. The difference in polym-

erization propagation mechanism compared to multifunctional acrylates results in a different temporal structure development. Gratings formed using this chemistry have a much different final morphology, exhibit better optical and electrooptical properties, and show better long-term stability. Future work will concentrate on the development of visible initiators to photopolymerize thiol-ene material systems using visible laser light.

Acknowledgment. The authors (L.V.N, R.L.S., and V.P.T) gratefully acknowledge the support of the Air Force through Contract F33615-99-C-5415 and AFOSR/NL. This work was performed at the Materials Directorate of Air Force Wright Laboratory, Wright-Patterson Air Force Base, and also at the Electrooptical Laboratory of SAIC located at Signal Hill, Dayton, OH.

CM021824D